

VIRTUAL SRF CAVITY: TESTING SRF CAVITY SUPPORT SYSTEMS WITHOUT THE HASSLE OF LIQUID HELIUM AND KLYSTRONS *

P. Echevarria[†], A. Neumann, A. Ushakov, J. Knobloch,
Helmholtz Zentrum Berlin, Berlin, Germany

E. Aldekoa, J. Jugo, University of the Basque Country (UPV/EHU), Leioa, Spain

Abstract

Setting up and debugging SRF support systems, such as LLRF control, quench detection, microphonics and Lorentz-force detuning control, etc., often requires extensive time spent operating the cavities. This results in time consuming and costly operation. Early into the development stages the actual cavity system may not even be available. It is therefore highly desirable to pre-evaluate these systems under realistic conditions prior to final testing with the SRF cavities. We devised an FPGA-based "virtual cavity" that takes a regular low-level RF input and generates the signals for RF-power reflection, transmission and detuning that mimic the response of a real cavity system. As far as the user is concerned, the response is the same as for a real cavity. This "black-box" model includes mechanical modes, Lorentz force detuning, a field depended quality factor, quenches and variable input coupling and is currently being expanded. We present the model and show some applications for operating the quench detection, LLRF and microphonics control for 1.3 GHz bERLinPro cavities. The same system can be used for other cavity types, including normal conducting cavities.

INTRODUCTION

The unavailability of SRF cavities and all the associated ancillary systems for testing them is a big issue when designing and debugging LLRF control algorithms and related techniques like quench detection, detuning compensation, etc. In [1] an FPGA-based virtual cavity was presented which could be used to perform hardware-in-the-loop (HIL) simulations of the mentioned systems. This system, based on off-the-shelf National Instruments hardware, takes the forward RF signal coming from the LLRF system and models the electrical behaviour of an SRF cavity generating the RF transmitted and reflected signals.

In addition to this basic electrical behaviour, some more advanced features were introduced to the model such as a quenching, field dependant Q and mechanical response fed by Lorentz force detuning and microphonics, making the system more realistic and close the real world.

In this paper all these components of the virtual cavity are summarized and a more modern and more compact hardware is presented, which allowed the introduction of one more feature: the simulation of the piezo tuner with its associated mechanical transfer function. The resulting system offers the operator the flexibility to choose between

different quality factors, couplings, quench thresholds, mechanical responses while the FPGA calculates in real time the transmitted and reflected RF voltages for a given RF input. Figure 1 depicts the overview of the working principle of this virtual cavity,

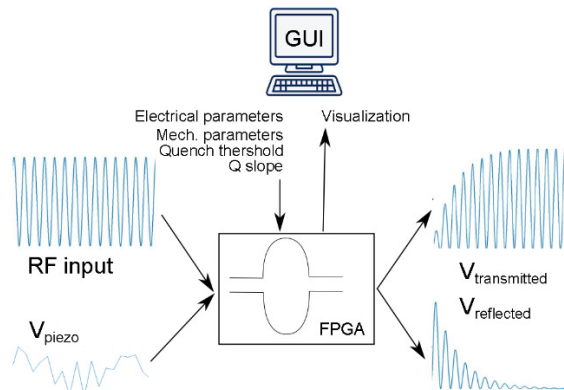


Figure 1: Overview of the virtual cavity operation scheme.

NEW HARDWARE

The hardware used in [1] was the main limitation to add more features to the virtual cavity as almost all the FPGA resources were used. Therefore the whole design was migrated to a newer and more compact device from National Instruments [2]. This device is composed by a real time controller in charge of the communications with the user via Ethernet and a Kintex-7 FPGA where the cavity model is implemented. The analog module was also changed, [3], in order to have more number of inputs and outputs, 16-bit ADCs and a bigger dynamic range. Figure 2 shows both devices.

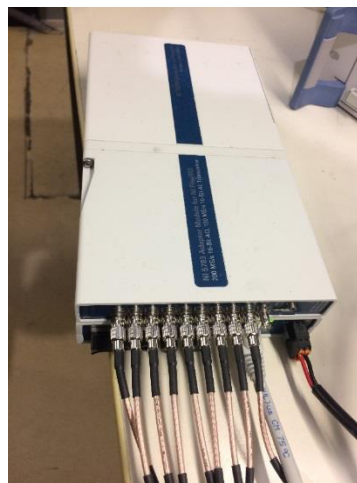


Figure 2: National Instruments NI-7935R FlexRIO controller, [2] with the NI-5783 Analog Adapter Module, [3].

* Work supported by German Bundesministerium für Bildung und Forschung, Land Berlin, grants of Helmholtz Association and partially supported by Basque Country PPG17/25 project.

[†] pablo.echevarria@helmholtz-berlin.de

Content from this work may be used under the terms of the CC BY 3.0 licence (© 2019). Any distribution of this work must maintain attribution to the author(s), title of the work, publisher, and DOI.

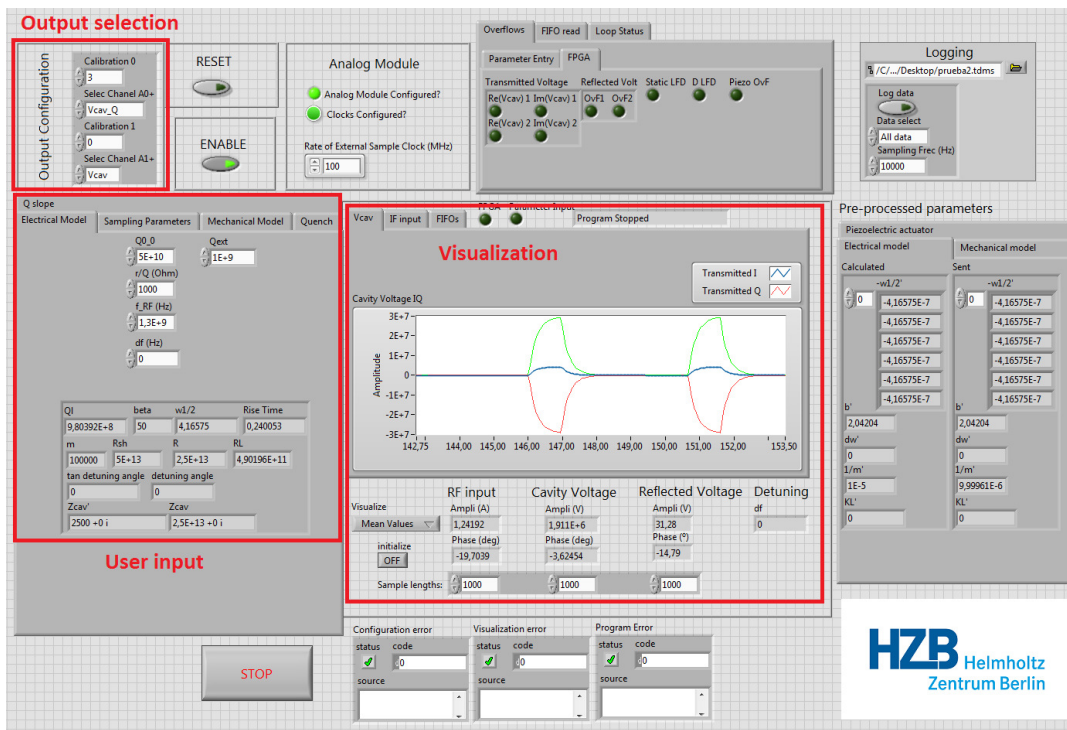


Figure 3: Graphical user interface where the parameter input, analog output selection and data visualization are depicted.

ELECTRICAL MODEL

The basic cavity electrical behaviour can be modelled using an equivalent RLC-circuit, [4], which leads to the following equation:

$$\frac{d}{dt} \mathbf{V}_{cav} = \begin{pmatrix} -\omega_{1/2} & -\Delta\omega \\ \Delta\omega & -\omega_{1/2} \end{pmatrix} \mathbf{V}_{cav} + \begin{pmatrix} R_L \omega_{1/2} & 0 \\ 0 & R_L \omega_{1/2} \end{pmatrix} \frac{\mathbf{I}_{amp}}{m} \quad (1)$$

where $\omega_{1/2}$ is the half bandwidth, $\Delta\omega$ the cavity detuning, R_L is the load resistance, m is the transformer ratio (both dependent on r/Q , Q_0 and the coupling factor) and $\mathbf{V}_{cav} = (V_{cav}^r, V_{cav}^i)$, $\mathbf{I}_{amp} = (I_{amp}^r, I_{amp}^i)$ are the real and imaginary parts of cavity voltage and the driven current respectively.

The reflected voltage is calculated with the following equation:

$$\mathbf{V}_{ref} = \frac{\mathbf{V}_{cav}}{m} - \frac{Z_0 \mathbf{I}_{amp}}{2} \quad (2)$$

where Z_0 is the impedance of the RF system (normally 50 ohm).

Equations (1) and (2), after a proper discretization, have been implemented in the FPGA, where the in-phase and in quadrature components of the input are obtained through an IQ-sampling block.

The user interface allows the introduction of the following parameters: r/Q , Q_0 , Q_{ext} , frequency, and detuning and

the program calculates all the derived variables as Q_L , coupling factor, half-bandwidth, rise time, etc. as it can be seen in Fig. 3. The range of these parameters are limited by the fixed point representation inside of the cavity and depend on each other. For instance at 1.3 GHz the minimum Q_L is around 1.75×10^5 and the maximum around 5×10^{11} .

MORE REALISTIC FEATURES

The utilization of an FPGA allows that the parameters in equations (1) and (2) are not only given by the user but also changed dynamically and in real time.

For instance the amplitude of the transmitted voltage can be calculated and used to change Q_0 to the minimum possible value when the field is above a threshold given by the user, simulating this way a quench of the SRF cavity. The amplitude can be also used to address a look-up table where different Q_0 values are stored and fed back to the cavity model, so the system presents a field dependent Q_0 .

Finally, the square of the amplitude value can be added to a signal coming from the host simulating microphonics and fed to a block that implements the mechanical transfer function of the cavity. Up to five mechanical eigenmodes can be set by the user defined by the natural frequency, ω_m , the quality factor, Q_m , and the coupling factor, K_m . Each of these mechanical modes are defined by:

$$\frac{d}{dt} \begin{pmatrix} \Delta\omega_m(t) \\ \Delta\dot{\omega}_m(t) \end{pmatrix} = \begin{pmatrix} 0 & 1 \\ -\omega_m^2 & \frac{\omega_m}{Q_m} \end{pmatrix} \begin{pmatrix} \Delta\omega_m(t) \\ \Delta\dot{\omega}_m(t) \end{pmatrix} + \begin{pmatrix} 0 \\ -K_m \omega_m^2 \end{pmatrix} (E_{cav}^2 + M_c) \quad (3)$$

Content from this work may be used under the terms of the CC BY 3.0 licence (© 2019). Any distribution of this work must maintain attribution to the author(s), title of the work, publisher, and DOI.

where E_{cav} is the electric field in the cavity and M_c is the microphonics signal coming from the host. The results of the five modes, $\Delta\omega_m(t)$, $m = 1, \dots, 5$ are added and fed as detuning to the cavity model, simulating this way the Lorentz force detuning plus microphonics. So far, four type of microphonics signals can be generated in the host: white noise, a sinusoidal signal with configurable amplitude and frequency, an impulse and a step function to simulate mechanical hits and displacements of the cavity.

PIEZO TUNER MECHANICAL MODEL

Since the newer hardware has more FPGA resources and inputs, the mechanical model of the piezo tuner has been implemented. In a similar way as in the previous section, five mechanical modes are implemented but this time they are fed by an external signal that simulates the voltage applied to the piezo stack of the tuner of an SRF cavity. In addition to the mechanical modes, to make this block more realistic, a DC component and a delay (to mimic the phase lag of the tuner) are introduced. The implemented transfer function is given by the following equation:

$$\frac{\Delta\omega(s)}{V_{piezo}(s)} = \left(\frac{M_0}{\tau s + 1} + \sum_{i=1}^5 \frac{\omega_i^2 M_i}{s^2 + \frac{\omega_i}{Q_i} s + \omega_i^2} \right) e^{-T_{delay} s} \quad (4)$$

where $\Delta\omega$ is the total detuning, V_{piezo} is the voltage applied at the analog input, M_i , ω_i , and Q_i are respectively the gains, resonant frequency and quality factor of each mode, τ is the parameter defining the dynamics of the DC component, and T_{delay} is the phase lag of the tuner.

Figure 4 shows the complete block diagram of the virtual cavity with this new feature. The detuning caused by the piezo driver is added to the one caused to the Lorentz force detuning and microphonics. In order to test that the new block works as intended a mechanical eigenmode at 40 Hz with a quality factor of 10 was set in the user interface and a sweep of the frequency at the analog input was done. Figure 5 shows the frequency response where it can be seen that frequency peak and bandwidth match with the introduced values. Figure 6 depicts the effect of the tuner phase lag.

EXAMPLES OF APPLICATIONS

For the LLRF operation of the Berlin's Energy Recovery Linac (bERLinPro), [5], the mTCA.4 standard is being used. The main items of the amplitude and phase control of this 1.3 GHz machine are a downconverter and vector modulator board connected to the rear of the crate, [6], and a digitizer and FPGA board, [7]. In order to connect the virtual cavity operating at an intermediate frequency with these high frequency elements, an up/downconverter is introduced as an interface both devices as it can be seen in Fig. 7. This setup is currently used at HZB to help to design and debug several aspects of the LLRF control of bERLinPro as it explained below.

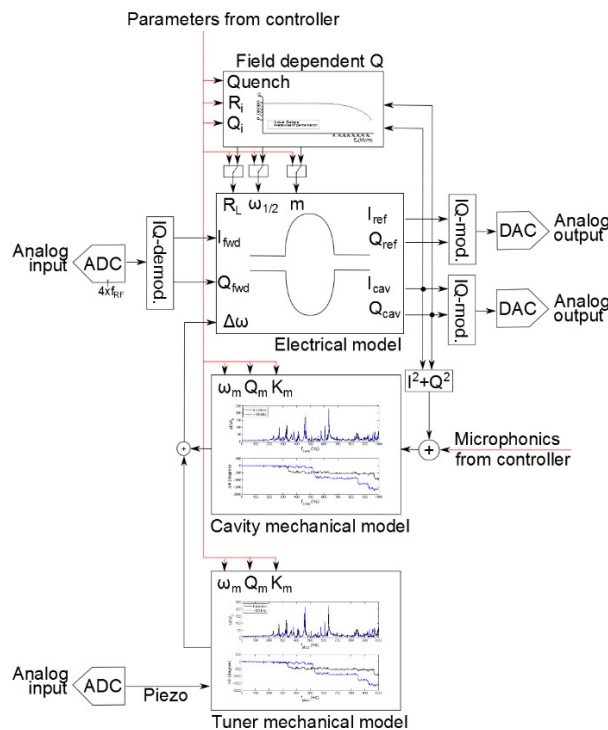


Figure 4: Block diagram of the implemented virtual cavity with the piezo tuner block.

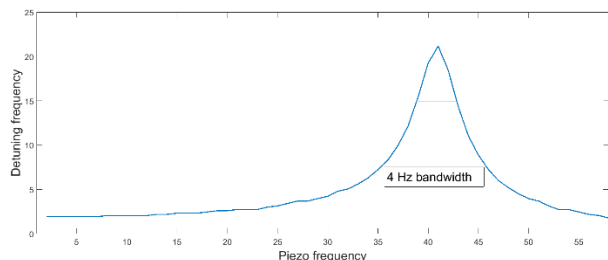


Figure 5: Frequency response of the piezo tuner mechanical block with an eigenmode at 40 Hz with a quality factor of 10.

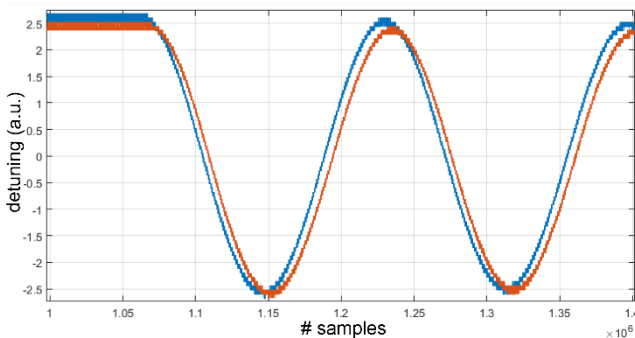


Figure 6: Piezo tuner mechanical response without (blue) and with a 50 ms phase lag (red) with a 10^{-7} s sampling period.

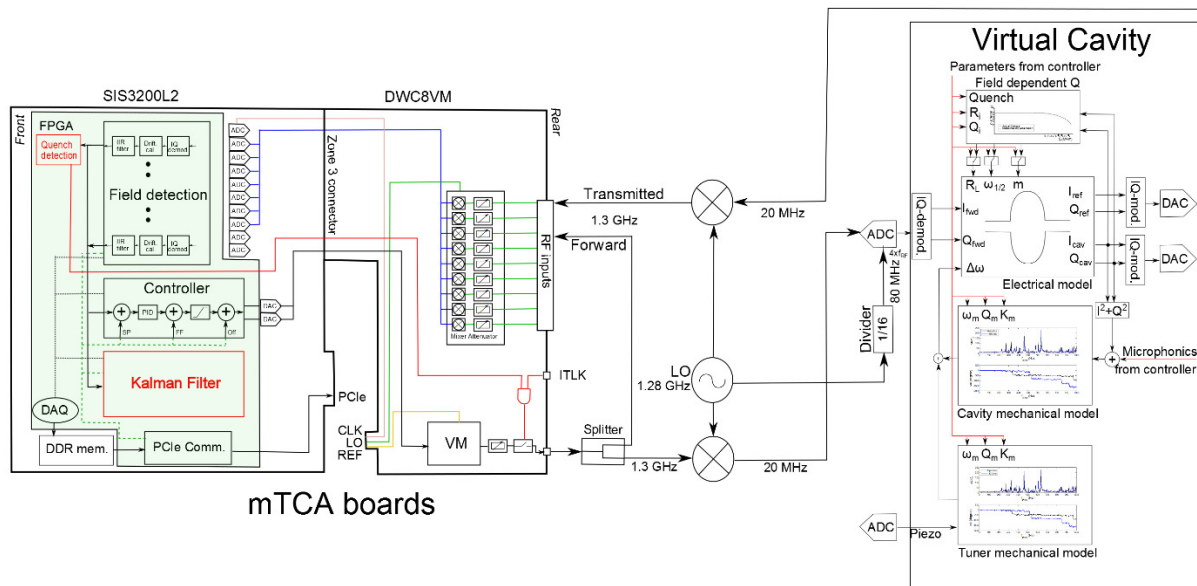


Figure 7: An Up/Downconverter has been used to convert the signals coming to and from the virtual cavity (center of the image) to enable the use of mTCA.4 boards (left).

Kalman Filter Estimator Testing and Debugging

The first application of the virtual cavity at HZB was done during testing and debugging of the optimal estimator for unresolved measurement implemented by the Kalman filter, [8]. The idea behind this technique is predict the detuning of a cavity due to microphonics when the mechanical behavior of the cavity is not properly described and/or when the system is noisy. The Kalman filter is able to deal with this uncertainties in iterative way, where in each step defines which value is more trustworthy: the theoretical response calculated using the measured mechanical transfer function or the real-time measured detuning of the cavity.

The virtual cavity has been used to debug the implementation of this filter (Fig. 7) for the following reasons:

- The system is known to generate parameterized signals describing real cavities with known behavior.
- Realistic behaviour can be emulated (Fig. 8).
- Different waveforms of the mechanical modes' input signals were examined including impulses with known amplitude and duration imitating the real processes (Fig. 9).
- Possibility to simulate the sum of several mechanical modes (Fig. 9).
- Additional noise was added to the input signals making it possible to check the response of the filter and examine filters margins.

Quench Detection Algorithms

The usual RF signals used as input for LLRF control, i.e. the transmitted and forward voltages, can be used to determine online the cavity parameters, [9]. If a sudden change in $\omega_{1/2}$ due to the drop of the quality factor of the cavity when quenching is detected, the LLRF system can immediately interlock the RF signal preventing the cavity and cryomodule to suffer any damage. This technique has

proven fast enough to detect a quench in the SRF cavities of the HZB projects (bERLinPro and BESSY-VSR, [10]) and switch off the RF before the deposited power in the He bath is too high, [11]. Following this year, this algorithm will be implemented in the mTCA.4 FPGA board and as a first step prior to be used in a real cavity, the virtual cavity's quench feature will be used to debug and adjust the algorithm.

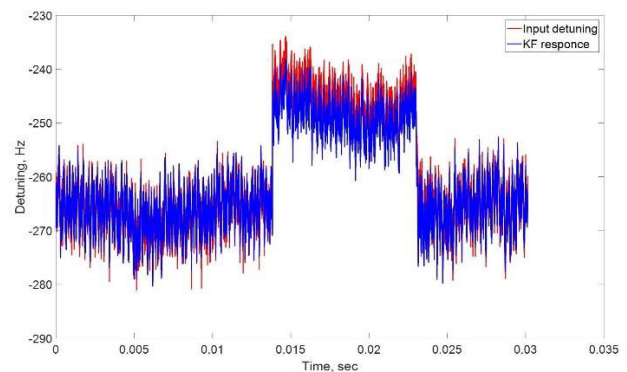


Figure 8: Detuning emulating the real processes of 1 mbar pressure change in LHe system or a non-synchronized beam injection into BESSY-II generated with the virtual cavity (red) and the Kalman filter estimation (blue).

bERLinPro LLRF Control Panels

The virtual cavity, connected to an mTCA.4 crate as in Fig. 7 has been used to debug and properly initialize the registers in the FPGA firmware. These registers, together with the DRAM memory of the board are accessed by the in-crate CPU through the PCIe bus in the backplane. The CPU runs the LLRF server developed by DESY to be used initially with the DOOCS control system [12], but with the use of the ChimeraTK Control System Adapter [13-14] it has been adapted to be connected to the EPICS control sys-

Content from this work may be used under the terms of the CC BY 3.0 licence (© 2019). Any distribution of this work must maintain attribution to the author(s), title of the work, publisher, and DOI.

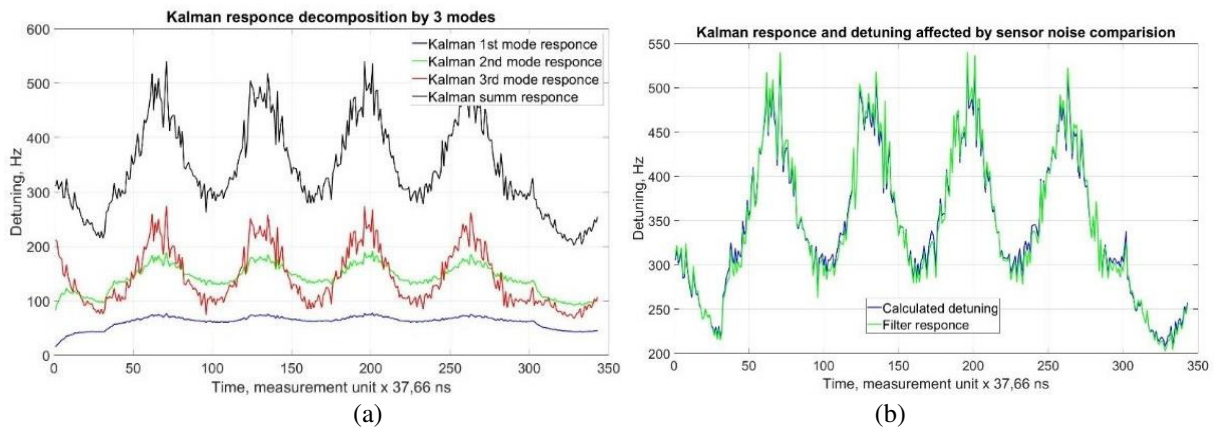


Figure 9: Composition of several mechanical modes of different shape, quality, coupling and noise. (a) shows decomposition of 3 mechanical modes 330, 460 and 470 Hz. (b) shows Kalman filter tracking ability for those mentioned signals.



Figure 10: Virtual cavity GUI (above) and LLRF EPICS panels (below) running in the same computer of the control room.

tem of HZB, [15].

This setup has been used to close the amplitude and phase control loops of the virtual cavity, and it has proven to be a very useful, fast and cheap way to learn how to use the control panels from an operator point of view without the risks of driving a real cavity with high power RF (Fig. 10).

CONCLUSIONS

The presented virtual cavity has proven to be a very useful tool for setting up and debugging LLRF systems without using a real cavity. This not only makes it possible when no cavity is available at all, but also allows to do it in a cheap (no cryogenics nor ultra-high vacuum needed) and safe manners (no radiation nor high power RF involved).

In addition to the testing of advanced techniques like the Kalman filter for mechanical detuning estimation or real-time detection of quenches, the virtual cavity combined with an up/down converter connected to an mTCA.4 chassis offers a non-dangerous setup to train the machine operator on the use of the control panels.

The presented new hardware with its modern FPGA still has enough resources to further implement more features. For instance, the electrical behaviour could be expanded to include pass-band modes of multicell cavities, or even several cavities can be implemented to emulate the vector sum operation of several cavities driven by a single RF amplifier, [16].

ACKNOWLEDGEMENTS

Authors would like Martin Hierholzer from DESY for his help setting up the LLRF server together with the ChimeraTK Control System Adapter.

REFERENCES

- [1] P. Echevarria, E. Aldekoa, J. Jugo, A. Neumann, A. Ushakov, and J. Knobloch, "Superconducting radio-frequency virtual cavity for control algorithms debugging", *Rev. Sci. Inst.*, vol. 89, no. 8, p. 084706, 2018. doi:10.1063/1.5041079
- [2] National Instruments, "The Controller for FlexRIO: A Deep Dive on Deployable Instrumentation", <http://www.ni.com>
- [3] NI 5783, <http://www.ni.com/pdf/manuals/375445a.pdf>
- [4] T. Schilcher, "Vector sum control of pulsed accelerating fields in Lorentz force detuned superconducting cavities", Ph.D. thesis, Hamburg University, 1998.
- [5] P. Echevarria, J. Knobloch, O. Kugeler, A. Neumann, K.P. Przygoda, and A. Ushakov, "First LLRF Tests of BERLinPro Gun Cavity Prototype", in *Proc. 7th Int. Particle Accelerator Conf. (IPAC'16)*, Busan, Korea, May 2016, paper TU-POW035, pp. 1831-1834, ISBN: 978-3-95450-147-2, doi:10.18429/JACoW-IPAC2016-TUPOW035, <http://jacow.org/ipac2016/papers/tupow035.pdf>
- [6] DWC8VM1 mTCA.4 Downconverter/Vector Modulator RTM, <https://www.struck.de/dwc8vm1.html>
- [7] SIS8300-L2 mTCA Digitizer advanced mezzanine card, <https://www.struck.de/sis8300-l2.html>

- [8] A. Ushakov, P. Echevarria, and A. Neumann, “Developing Kalman Filter Based Detuning Control with a Digital SRF CW Cavity Simulator”, in *Proc. 9th Int. Particle Accelerator Conf. (IPAC'18)*, Vancouver, BC, Canada, Apr. 4., pp. 2114-2117, doi: 10.18429/JACoW-IPAC2018-WEPAK012
- [9] R. Rybaniec *et al.*, “Real time estimation of superconducting cavities parameters”, in *Proc. 5th Int. Particle Accelerator Conf. (IPAC'14)*, Dresden, Germany, June 2014, pp. 2456-2458. doi: 10.18429/JACoW-IPAC2014-WEPME075
- [10] P. Schnizer *et al.*, “Status of the BESSY VSR Project”, in *Proc. 9th Int. Particle Accelerator Conf. (IPAC'18)*, Vancouver, BC, Canada, Apr. 4., pp. 4138-4141, doi: 10.18429/JACoW-IPAC2018-THPMF038
- [11] P. Echevarria, A. Neumann, A. Ushakov, B. Garcia Arruabarrena, and J. Jugo, “Simulation of quench detection algorithms for Helmholtz Zentrum Berlin”, *J. Phys. Conf. Ser.*, to be published.
- [12] The Distributed Object Oriented Control System (DOOCS), <http://doocs.desy.de/>
- [13] ChimeraTK: Control system and Hardware Interface with Mapped and Extensible Register-based device Abstraction Tool Kit, <https://github.com/ChimeraTK/>
- [14] M. Killenberg *et al.*, “Abstracted Hardware and Middleware Access in Control Applications”, in *Proc. 16th Int. Conf. on Accelerator and Large Experimental Control Systems (ICALEPCS'17)*, Barcelona, Spain, Oct. 2017, paper TUPHA178, pp. 840-845, ISBN: 978-3-95450-193-9, <https://doi.org/10.18429/JACoW-ICALEPCS2017-TUPHA178>, 2018.
- [15] Experimental Physics and Industrial Control System (EPICS), <http://www.aps.anl.gov/epics/index.php>
- [16] J. Branlard *et al.*, “The European LLRF system”, in *Proc. 3th Int. Particle Accelerator Conf. (IPAC'12)*, New Orleans, USA, May 2012, pp. 55-57.